# Exploration of Thermal Bridging through Shrub Branches 1 in Alpine Snow

Florent Domine, Kévin Fourteau, P. Choler

# Exploration of Thermal Bridging through Shrub Branches in Alpine Snow

**Florent Domine[1,2,3*], Kevin Fourteau[4*], and Philippe Choler[5]**

[1] Takuvik Joint International Laboratory, Université Laval (Canada) and CNRS-INSU (France), Québec, Canada.

[2] Centre d'Études Nordiques, Université Laval, Québec, Canada.

[3] Department of Chemistry, Université Laval, Québec, Canada.

[4] Univ. Grenoble Alpes, Univ. Toulouse, Météo-France, CNRS, CNRM, Centre d'Études de la Neige, Grenoble, France

[5] Univ. Grenoble Alpes, Univ. Savoie Mont Blanc, CNRS, LECA, Grenoble, France

Corresponding author: Florent Domine. *e-mail*: florent.domine@gmail.com

*These authors contributed equally to this work.

**Key Points:**

- The winter ground temperature in a snow-covered alpine area during a cold spell is 1.3°C colder under alders than under nearby grass.
- Using finite element modeling, we demonstrate that this is due to thermal bridging through alder branches.
- Plane-parallel snow layer geometry cannot be used to model ground temperature, soil freezing, and snow metamorphism if shrubs are present.

## Abstract

In the high Arctic, thermal bridging through frozen shrub branches has been demonstrated to cool the ground by up to 4°C during cold spells, affecting snow metamorphism and soil carbon and nutrients. In alpine conditions, the thermal conductivity contrast between shrub branches and snow is much less than in the Arctic, so that the importance of thermal bridging is uncertain. We explore this effect by monitoring ground temperature and liquid water content under green alders and under nearby alpine tundra in the Alps. During a January 2022 cold spell, the ground temperature at 5 cm depth under alders is 1.3°C colder than under alpine tundra. Ground water freezing under alders is complete, while water remains liquid under tundra. Finite element simulations reproduce the observed temperature difference between both sites, showing that thermal bridging does affect ground temperature also under Alpine conditions.



## Plain Language Summary

With climate warming, shrubs are expanding in seasonally snow-covered Arctic and alpine areas. In the Arctic, it has been shown that shrubs buried in snow act as thermal bridges between the ground and the atmosphere, so that the ground winter temperature is colder than if thermal effects due to snow only are considered. Thermal bridging is efficient in the Arctic because the thermal conductivity of shrub branches is 30 to 70 times as large as that of snow. In alpine areas, the difference in thermal conductivity between the shrub branches and the snow is much lower, so that the efficiency of thermal bridging by shrubs is uncertain, even though shrub branches are much thicker. We monitored the soil temperature at an Alpine site at a spot with green alders and a nearby spot with herbaceous vegetation. The ground was 1.3°C colder under alders during a cold spell. Using finite element simulations, we show that this is explained by thermal bridging through alder branches. Snow and land surface models must therefore include this process for adequate simulations of the soil temperature, soil freezing and carbon recycling, snow metamorphism and snow physical properties.

## 1 Introduction

In snow-covered areas, heat exchanges between the atmosphere and the ground through the snowpack determine winter ground temperature (Domine et al., 2019). Physical snow models describe heat exchanges through snowpacks based on a plane-parallel snow layer geometry. In Arctic and Alpine areas, shrubs are expanding (Anthelme et al., 2003; Wiedmer & Senn-Irlet, 2006; Ju & Masek, 2016), inducing changes in snow properties. Shrubs trap blowing snow, increasing snow height (Sturm et al., 2001; Lamare et al., 2023), reducing snow compaction, and favoring the formation of the most thermally-insulating snow type: depth hoar (Domine, Barrere, & Morin, 2016).. Furthermore, shrub branches disrupt the plane-parallel geometry. Recently, thermal bridging through frozen shrub branches buried in snow has been detected in the high Arctic (Domine et al., 2022), enhancing ground cooling in winter, despite widespread depth hoar. Cooling averaged over the November-February period was 1.21°C, but reached 4°C during cold spells. Accurate simulation of the ground temperature by snow models is crucial as it impacts the temperature gradient in the snowpack, which determines metamorphism and snow physical properties. Ground temperature is equally important to land surface models to simulate carbon and nutrient recycling in soils, which considerably slows down when the ground freezes (Saccone et al., 2013).

In the Arctic, the thermal conductivity contrast between snow found in shrubs and frozen shrub branches is a factor of 30 to 70. Snow within shrubs is mostly depth hoar with a thermal conductivity of 0.03 to 0.07 $Wm^{-1}K^{-1}$ in the Arctic (Domine, Barrere, & Morin, 2016; Domine et al., 2022) while the thermal conductivity of frozen wood is around 2 $Wm^{-1}K^{-1}$ (Domine et al., 2022). Therefore, even though high Arctic shrub branches rarely exceed 3 cm in diameter (Sturm et al., 2001; Domine et al., 2022), the thermal conductivity contrast is sufficient for thermal bridging through frozen shrub branches to efficiently cool the ground.

Whether thermal bridging also operates in Alpine regions is uncertain because the thermal contrast between alpine snow and the presumably unfrozen alpine shrub branches is much less than in the Arctic. (Morin et al., 2010), (Calonne et al., 2011) and (Riche & Schneebeli, 2013) measured thermal conductivity values from 0.05 to 0.46 $Wm^{-1}K^{-1}$ for Alpine snow. These values were however for snow without shrubs, whose effects are therefore not considered.

Snow temperature in Alpine regions where shrubs are found seldom drop durably below -10°C (Morin et al., 2010; Morin et al., 2012). At these temperatures, shrub branches probably do not freeze because of physiological freeze resistance (Squeo et al., 1996; Zhang et al., 2016). The axial thermal conductivity of fresh wood is 0.5 to 1 $W\ m^{-1}\ K^{-1}$, with the higher values more frequent (Turrell et al., 1967; Deliiski, 2013; Laguela et al., 2015). The thermal contrast between snow and buried shrub branches in Alpine regions is therefore in the range 1 to 20, much less than in the Arctic. Alpine shrub branches are however much bigger than in the Arctic, e.g.green alders (*Alnus alnobetula*) have branches up to 10 cm in diameter (Wiedmer & Senn-Irlet, 2006). The cross-sectional surface area of shrub branches may therefore be at least a factor of 10 greater than in the Arctic, compensating the lower thermal conductivity contrast.

Thermal bridging through shrub branches buried in Alpine snow therefore deserves investigation. This preliminary study of the process explores whether a more complete study with extensive instrumental deployment is justified. We report data from the 2021-2022 winter near the Col du Lautaret, French Alps. Using finite element modeling, we conclude that thermal bridging through shrub branches is necessary to explain observations. More detailed studies of thermal bridging in Alpine conditions are therefore warranted.

## 2 Materials and Methods

### 2.1 Species and site description

The green alder, *Alnus alnobetula* , is a tall deciduous shrub growing up to 5-6 m. It exhibits clonal growth with many ascending branches, which sprout from a horizontal thickened stem. In the Alps, green alders form dense stands in many north-exposed slopes between 1000 m and 2000 m (Richard, 1968; Wiedmer & Senn-Irlet, 2006). The estimated above-ground biomass of dense *Alnus* stands amounts 100 t $ha^{-1}$ (Richard, 1968), much more than in the Arctic, where values around 10 and 2 t $ha^{-1}$ have been estimated in the low and high Arctic, respectively (Greaves et al., 2016; Paradis et al., 2016). Over the recent decades, the green alder has been expanding at the expense of formerly grazed grasslands (Figure S1 in supporting information), affecting biodiversity (Anthelme et al., 2003).

The study site (45.034750°N, 6.413630°E, 2034 m asl), called Alnus-Nivus, is a north-facing slope dominated by green alders up to 2.5 m tall (Figure 1 and Figure S2 in Supporting Information). It is located within a nature reserve so that placing visible instruments is not permitted. Only buried sensors could be deployed. The site was selected because of the presence of the nearby FR-Clt meteorological station (45.041278°N, 6.410611°E, 2046 m asl, (Gupta et al., 2023)) about 750 m away on a 4° south-facing slope across the valley, where there is no alder, and which is outside the nature reserve. This station is part of the Integrated Carbon Observation System network (https://www.icos-cp.eu/observations/ecosystem/stations).

### 2.2 Instruments

We placed 5TM temperature and fractional volume water content sensors from Decagon in the ground at 5 and 15 cm depths at two spots: (i) under a green alder, near the emergence of ascending branches, hereafter called ALNUS; and (ii) in a nearby grass patch about 6 m away, hereafter called GRASS. Values of air temperature, wind speed and downwelling longwave radiation measured at FR-Clt are probably reasonably similar to those at Alnus-Nivus. However, downwelling shortwave radiation is significantly different in winter because the site is entirely shaded by mountains. Snow height is higher at Alnus-Nivus. On 31 March 2021, we measured over 1.5 m of snow at both ALNUS and GRASS vs only 0.5 m at the FR-Clt station.

### 2.3 Field measurements

On 19 September 2022, we measured the ground thermal conductivity at 5 and 15 cm depths at ALNUS and GRASS using a TP02 heated needle probe from Hukseflux, as described in (Domine et al., 2015). At ALNUS, we counted a total of 35 primary branches at 50 cm height,

with a mean diameter of 6.5 cm. No winter measurements were performed because of the avalanche risk.

### 2.4 Finite element model calculations

Heat transfer between snow, soil, and shrub branches was simulated with finite element modeling, using the open source ElmerFEM software (Malinen & Råback, 2013), as detailed in (Domine et al., 2022). The shrub geometry used, based on field observations, is shown in Figure 2. Branches were constructed only to a height of 1 m, greater than the 0.7m snow height. All branches were 6.5 cm in diameter, the average measured. Secondary branches were omitted. The wood density and specific heat values were 900 kg $m^{-3}$ and 1200 J $kg^{-1}$ $K^{-1}$ (Radmanovic et al., 2014). Since measured soil thermal conductivities were different at ALNUS and GRASS (Table S1 in Supporting Information), we divided the ground between an ALNUS ground with a radius of 0.75 m around the shrub, and a GRASS ground beyond that. The soil comprised three layers: 0-8 cm, 8-30 cm, and 30 cm to 10 m (Figure 2 and Table S1). For frozen soil, measured values were multiplied by two (Table S1), following measurements in the Arctic (Domine, Barrere, & Sarrazin, 2016; Domine et al., 2022). The baseline soil volumetric thermal capacity used was 2.6 x $10^6$ J $m^{-3}$ $K^{-1}$, corresponding to a density of 1300 kg $m^{-3}$ and a specific heat of 2000 J $K^{-1}$ $kg^{-1}$. To represent the effect of water phase change on temperature, a Soil Freezing Characteristic Curve (SFCC) was used under the form of an increased apparent thermal capacity (Tubini et al., 2021). In practice, the thermal capacity of the soil was increased near the freezing point, accounting for the extra-energy needed to change the soil temperature just below 0°C, as a fraction of the energy is converted to latent rather than sensible heat. For instance, warming the soil from -1°C to 0°C requires an extra 9.1x$10^6$ J $m^{-3}$ of energy, compared to 2.6x$10^6$ J $m^{-3}$ if no freezing occurs. The SFCC was derived from water content versus temperature data measured at a tundra site at Bylot Island (Domine, Barrere, & Sarrazin, 2016; Domine et al., 2021). The soil there was silt loam, reasonably similar to that at ALNUS, based on observations on 19 September 2022.

A time-constant snow height was used for all simulations. The Gmsh software (Geuzaine & Remacle, 2009) was used to generate the finite element mesh. The simulations were run with a 30 min time step and forced at the top with the snow surface temperature, obtained from the longwave upwelling radiation measured at FR-Clt, using an emissivity of 1, and with the mean annual air temperature at 10 m depth, 3°C. Simulations ouputs used were temperatures in the vicinity (representing ALNUS) and away (representing GRASS) from the alder recorded at 5 and 15 cm depths, as shown in the bottom panel of Figure 2.

## 3 Results and discussion

### 3.1 Detection of thermal bridging from observations

Permanent snow cover at FR-Clt started on 25 November. Snow height exceeded 10 cm on 2 December 2021 and was 25 cm around 8 December (Figure 3). Snow height then varied between 30 and 70 cm, while the air temperature was often above 0°C and seldom dropped

below -10°C (Figure 3). The snow surface temperature dropped below -20°C on 3 December and was often below –15°C. Temperatures are shown in Figure 3 as 24 h running means for clarity.

Measured ground temperatures and ground liquid water contents at 5 and 15 cm depths are shown in Figure 4. These data inform us on sensible and latent heat fluxes between the ground and the atmosphere through the snow. Our analysis focuses on the period with permanent snow cover, starting on 1 December 2021.

Striking features in Figure 4 include: (1) cooling stages at ALNUS in early January and March (Figure 4a,b), indicating large sensible heat losses at ALNUS, with no sensible heat losses at GRASS; (2) large rapid changes in liquid water content at ALNUS in early December, late December and early January (Figure 4c,d), indicating large latent heat exchanges at ALNUS, with much lower and/or much slower exchanges at GRASS. ALNUS is thus clearly closely coupled to atmospheric temperature changes, while this coupling is much weaker at GRASS. This is consistent with an extra heat transport process existing at ALNUS. We hypothesize that thermal bridging through frozen shrub branches is that process. We detail two selected events.

A cold spell started on 4 January 2022 (Figure 3), with the air and snow surface temperatures dropping below 0°C. The daily-averaged snow surface temperature then remained below -5°C during 30 days. Figure 4 shows that at 5 cm depth at GRASS, the liquid water content and the ground temperature remained essentially unchanged throughout January, indicating little sensible or latent heat changes, probably because the limited heat loss through the insulating snowpack was compensated by the upward ground heat flux. At ALNUS however, most of the ground water froze rapidly on 6-7 January, indicating significant latent heat loss. Once most of the water was frozen, the ground temperature dropped below 0°C, and the sensible heat loss is clearly visible in Figures 4a and 4b, starting on 8 January.

Warming events also show much faster heat exchanges at ALNUS. The warming spell that started on 28 December led to the melting of essentially all the frozen ground water at ALNUS (Figures 4c,d), while only a small amount of frozen water melted at GRASS. Latent heat exchanges are thus much greater at ALNUS, and these exchanges most likely took place by heat transfer through the shrub branches.

Changes are similar at 15 cm depth, albeit slower because of the greater thermal inertia in deeper ground. At GRASS, the ground temperature remained at 0°C, while most of the water remained liquid. At ALNUS on the contrary, most of the water froze during cold spells and the temperature dropped to -0.7°C.

The extra sensible and latent heat exchanges at ALNUS at both depths may therefore reasonably be assigned to thermal bridging through snow. We test this hypothesis using finite element calculations.

### 3.2 Confirmation of thermal bridging by simulations

Finite element simulations were performed starting on 10 December to avoid the low and variable snow height in early December. Simulations were first performed with 70 cm of snow because we observed thicker snow at Alnus-Nivus than at FR-Clt. We used a snow thermal

conductivity value of 0.1 $Wm^{-1}K^{-1}$, so that the wood/snow thermal conductivity contrast is a factor of 10. We first performed simulations without shrubs to ensure that the different ground properties at ALNUS and GRASS were not responsible for observations. Ground thermal property differences do result in a cooler ground at ALNUS (Figure 5a), but by only 0.25°C and only for two short periods, insufficient to explain measurements. Figures 5b and 5c reproduce the data of Figure 4 reasonably well, given the simplifications. The GRASS temperatures remain close to 0°C, while those at ALNUS drop during the cold spells, to values identical to those measured. Despite the use of a SFCC for the soil, the zero-curtain effect is not as marked in simulations as in measurements, probably because of differences in SFCCs at Alvus-Nivus and at Bylot. Figures 5a to 5c demonstrate that including thermal bridging through shrub branches adequately simulates results.

Since snow height was not measured at Alnus-Nivus, we performed simulations for snow heights of 35 and 140 cm. Results are shown in Figure S3. As expected, thinner snow leads to in general colder ground while thicker snow leads to reduced cooling. However, qualitatively, results are similar, with a better thermal coupling between snow and ground at ALNUS, due to thermal bridging.

A higher snow thermal conductivity reduces the relative impact of thermal bridging. Figure S4 in Supplementary Information shows simulations with a snow thermal conductivity of 0.2 $Wm^{-1}K^{-1}$. Expectedly, the temperature difference between ALNUS and GRASS decreases, but the general trends are still reasonably reproduced.

Branch diameter and thermal conductivity also affect heat exchanges. Figure S5 shows results with 70 cm of snow of thermal conductivity 0.1 $Wm^{-1}K^{-1}$, and branches of 32, 65 and 130 mm diameter. Obviously, thicker branches increase the temperature difference between ALNUS and GRASS, confirming that thermal bridging strongly affects the temperature at ALNUS.

Alternative scenarios to shrub thermal bridging were explored to explain measurements. Reduced snow height at ALNUS would increase atmosphere-ground thermal coupling there. We performed simulations without shrubs, with only 35 cm of snow at ALNUS and snow height increasing to 70 cm towards the edge of the simulation domain (Figure S5). Figure 5d shows that results at ALNUS are in fact reasonably similar to those of Figure 5b. However, daily temperature variations are visible, while they do not appear in the data (Figure 4a) indicating that the thermal insulance of the snowpack is too low to realistically simulate the data. Furthermore, general observations indicate that the effect of shrub on snow height is rather to increase it, not to decrease it (Sturm et al., 2001; Busseau et al., 2017; Lamare et al., 2023). Moreover, snow height was not lower at ALNUS than at GRASS on 31 March 2021. The scenario of Figure 5d therefore appears unrealistic. Thermal bridging through alder branches is therefore the most reasonable explanation for the temperature difference between ALNUS and GRASS, and for the close thermal coupling between ALNUS and the atmosphere.

### 3.3 Upscaled impact and implementation in models

We calculated the impact of heat exchange through shrubs at the km scale by assuming a shrub density of one alder per square of 2x2m. By calculating the spatially-averaged heat flux

with and without shrubs, we find that the average thermal insulance decreases from 7 to 5.9 K $m^2 W^{-1}$ when shrubs are added. Alders represented in Figure 2, with a 70 cm snowpack, thus increase the heat flux through the snowpack by 15%. It is not possible to translate this directly into a temperature change because in most Alpine areas the soil temperature is usually near 0°C, meaning that latent heat exchanges are important, so that much of the flux will serve to freeze soil water. Soil freezing considerably reduces nutrient recycling and favors carbon accumulation (Saccone et al., 2013). Given that green alders are now quite widespread in the French Alps (Figure S7), the impact may be quite large and deserves evaluation.

In snow models, shrub thermal effects may be implemented simply by adjusting the thermal insulance of the snowpack to account for the increased heat flux. A more sophisticated approach would introduce shrubs as an extra domain that thermally couples the atmosphere and the soil. However, shrubs also affect radiation transfer in snowpacks (Belke-Brea et al., 2021), affecting snow temperature and metamorphism. Fully accounting for shrub effects would therefore require significant model modifications. The efforts are probably worthwhile, because shrubs keep expanding and adequate simulations of soil temperature are required for carbon budgets and productivity modeling (Loranty et al., 2018).

## 4 Conclusion

Field measurements and finite-element simulations lead to the conclusion that ground temperature under green alders is affected by thermal bridging through branches. Relative to the high Arctic, the lower thermal conductivity contrast between snow and branches is compensated by the greater branch cross section; 1095 $cm^2$ per simulated shrub here vs 92 $cm^2$ in the Arctic (Domine et al., 2022). Thermal bridging through shrub branches buried in snow is therefore probably a general process. Given the ever-greater shrub expansion in seasonally snow-covered areas, this process must be considered in snow physics models to accurately describe the thermal gradient in snowpacks, snow metamorphism and snow physical properties.

Thermal bridging also affects the thermal regime of the ground and here causes extensive ground freezing. This strongly affects microbial metabolism and therefore the carbon budget of soils, nutrient recycling and primary productivity (Saccone et al., 2013). These widespread effects justify further detailed study where all relevant meteorological, snow and soil variables are measured.

## Acknowledgements

This work was funded by NSERC (discovery grant to FD). KF was supported by the European Research Council (ERC) under the European Union's Horizon 2020 research and innovation program (IVORI grant 949516). Meteorological data are from the FR-Clt station, associated to the ICOS Ecosystem station network, and funded by labex OSUG@2020 and Jardin du Lautaret. We thank the staff of Jardin du Lautaret, in particular Pascal Salze and Lucie Liger, for logistical support.

## Open Research

The meteorological and soil data shown in Figure 3 and 4, as well as the simulation framework including the shrub mesh of Figure 2, are available on the Zenodo repository at https://doi.org/10.5281/zenodo.8057992, (Domine et al., 2023).

## References


Anthelme, F., Michalet, R., Barbaro, L., & Brun, J. J. (2003). Environmental and spatial influences of shrub cover (Alnus viridis DC.) on vegetation diversity at the upper treeline in the inner western Alps. *Arctic Antarctic and Alpine Research, 35*(1), 48-55. http://dx.doi.org/10.1657/1523-0430(2003)035[0048:Easios]2.0.Co;2

Belke-Brea, M., Domine, F., Picard, G., Barrere, M., & Arnaud, L. (2021). On the influence of erect shrubs on the irradiance profile in snow. *Biogeosciences, 18*(21), 5851-5869. https://bg.copernicus.org/articles/18/5851/2021/

Busseau, B.-C., Royer, A., Roy, A., Langlois, A., & Domine, F. (2017). Analysis of snow-vegetation interactions in the low Arctic-Subarctic transition zone (northeastern Canada). *Physical Geography, 38*(2), 159-175. http://dx.doi.org/10.1080/02723646.2017.1283477

Calonne, N., Flin, F., Morin, S., Lesaffre, B., du Roscoat, S. R., & Geindreau, C. (2011). Numerical and experimental investigations of the effective thermal conductivity of snow. *Geophysical Research Letters, 38*, L23501. <Go to ISI>://WOS:000297635100001

Deliiski, N. (2013). Computation of the wood thermal conductivity during defrosting of the wood. *Wood Research, 58*(4), 637-649. http://www.woodresearch.sk/wr/201304/13.pdf

Domine, F., Barrere, M., & Morin, S. (2016). The growth of shrubs on high Arctic tundra at Bylot Island: impact on snow physical properties and permafrost thermal regime. *Biogeosciences, 13*(23), 6471-6486. http://www.biogeosciences.net/13/6471/2016/

Domine, F., Barrere, M., & Sarrazin, D. (2016). Seasonal evolution of the effective thermal conductivity of the snow and the soil in high Arctic herb tundra at Bylot Island, Canada. *The Cryosphere, 10*(6), 2573-2588. http://www.the-cryosphere.net/10/2573/2016/

Domine, F., Barrere, M., Sarrazin, D., Morin, S., & Arnaud, L. (2015). Automatic monitoring of the effective thermal conductivity of snow in a low-Arctic shrub tundra. *The Cryosphere, 9*(3), 1265-1276. http://www.the-cryosphere.net/9/1265/2015/

Domine, F., Fourteau, K., Choler, P., & Voisin, D. (2023). *Soil and meteorological data, and finite element simulation framework for heat transfer through shrubs in winter near Lautaret pass, French Alps.* [Dataset] Zenodo. https://doi.org/10.5281/zenodo.8057992

Domine, F., Fourteau, K., Picard, G., Lackner, G., Sarrazin, D., & Poirier, M. (2022). Permafrost cooled in winter by thermal bridging through snow-covered shrub branches. *Nature Geoscience, 15*, 5540-5560. https://doi.org/10.1038/s41561-022-00979-2

Domine, F., Lackner, G., Sarrazin, D., Poirier, M., & Belke-Brea, M. (2021). Meteorological, snow and soil data (2013–2019) from a herb tundra permafrost site at Bylot Island, Canadian high Arctic, for driving and testing snow and land surface models. *Earth Syst. Sci. Data, 13*(9), 4331-4348. https://essd.copernicus.org/articles/13/4331/2021/

Domine, F., Picard, G., Morin, S., Barrere, M., Madore, J.-B., & Langlois, A. (2019). Major Issues in Simulating Some Arctic Snowpack Properties Using Current Detailed Snow Physics Models: Consequences for the Thermal Regime and Water Budget of Permafrost. *Journal of Advances in Modeling Earth Systems, 11*(1), 34-44. https://agupubs.onlinelibrary.wiley.com/doi/abs/10.1029/2018MS001445

Geuzaine, C., & Remacle, J.-F. (2009). Gmsh: A 3-D finite element mesh generator with built-in pre- and post-processing facilities. *International Journal for Numerical Methods in Engineering, 79*(11), 1309-1331. https://onlinelibrary.wiley.com/doi/abs/10.1002/nme.2579

Greaves, H. E., Vierling, L. A., Eitel, J. U. H., Boelman, N. T., Magney, T. S., Prager, C. M., & Griffin, K. L. (2016). High-resolution mapping of aboveground shrub biomass in Arctic tundra using airborne lidar and imagery. *Remote Sensing of Environment, 184*, 361-373. http://dx.doi.org/10.1016/j.rse.2016.07.026

Gupta, A., Reverdy, A., Cohard, J. M., Hector, B., Descloitres, M., Vandervaere, J. P., et al. (2023). Impact of distributed meteorological forcing on simulated snow cover and hydrological fluxes over a mid-elevation

alpine micro-scale catchment. *Hydrology and Earth System Sciences, 27*(1), 191-212. https://hess.copernicus.org/articles/27/191/2023/

Ju, J. C., & Masek, J. G. (2016). The vegetation greenness trend in Canada and US Alaska from 1984-2012 Landsat data. *Remote Sensing of Environment, 176*, 1-16. http://dx.doi.org/10.1016/j.rse.2016.01.001

Laguela, S., Bison, P., Peron, F., & Romagnoni, P. (2015). Thermal conductivity measurements on wood materials with transient plane source technique. *Thermochimica Acta, 600*, 45-51. http://dx.doi.org/10.1016/j.tca.2014.11.021

Lamare, M., Domine, F., Revuelto, J., Pelletier, M., Arnaud, L., & Picard, G. (2023). Investigating the Role of Shrub Height and Topography in Snow Accumulation on Low-Arctic Tundra using UAV-Borne Lidar. *Journal of Hydrometeorology, 24*(5), 835-853. https://journals.ametsoc.org/view/journals/hydr/24/5/JHM-D-22-0067.1.xml

Loranty, M. M., Abbott, B. W., Blok, D., Douglas, T. A., Epstein, H. E., Forbes, B. C., et al. (2018). Reviews and syntheses: Changing ecosystem influences on soil thermal regimes in northern high-latitude permafrost regions. *Biogeosciences, 15*(17), 5287-5313. https://dx.doi.org/10.5194/bg-15-5287-2018

Malinen, M., & Råback, P. (2013). Elmer Finite Element Solver for Multiphysics and Multiscale Problems. In I. Kondov & G. Sutmann (Eds.), *Multiscale Modelling Methods for Applications in Materials Science* (pp. 101–113). Jülich: Forschungszentrum Jülich GmbH.

Morin, S., Domine, F., Arnaud, L., & Picard, G. (2010). In-situ measurement of the effective thermal conductivity of snow. *Cold Regions Science and Technology, 64*, 73-80. http://dx.doi.org/10.1016/j.coldregions.2010.02.008

Morin, S., Lejeune, Y., Lesaffre, B., Panel, J. M., Poncet, D., David, P., & Sudul, M. (2012). An 18-yr long (1993–2011) snow and meteorological dataset from a mid-altitude mountain site (Col de Porte, France, 1325 m alt.) for driving and evaluating snowpack models. *Earth Syst. Sci. Data, 4*(1), 13-21. http://www.earth-syst-sci-data.net/4/13/2012/

Paradis, M., Lévesque, E., & Boudreau, S. (2016). Greater effect of increasing shrub height on winter versus summer soil temperature. *Environmental Research Letters, 11*(8), 085005. http://stacks.iop.org/1748-9326/11/i=8/a=085005

Radmanovic, K., Dukic, I., & Pervan, S. (2014). Specific Heat Capacity of Wood. *Drvna Industrija, 65*(2), 151-157. http://dx.doi.org/10.5552/drind.2014.1333

Richard, L. (1968). *Écologie de L'aune Vert (Alnus viridis): Facteurs Climatiques et édaphiques*. Retrieved from Grenoble: http://ecologie-alpine.ujf-grenoble.fr/articles/DCVA_1968__6__107_0.pdf

Riche, F., & Schneebeli, M. (2013). Thermal conductivity of snow measured by three independent methods and anisotropy considerations. *The Cryosphere, 7*(1), 217-227. http://www.the-cryosphere.net/7/217/2013/

Saccone, P., Morin, S., Baptist, F., Bonneville, J.-M., Colace, M.-P., Domine, F., et al. (2013). The effects of snowpack properties and plant strategies on litter decomposition during winter in subalpine meadows. *Plant and Soil, 363*, 215-229. http://dx.doi.org/10.1007/s11104-012-1307-3

Squeo, F. A., Rada, F., Garcia, C., Ponce, M., Rojas, A., & Azocar, A. (1996). Cold resistance mechanisms in high desert Andean plants. *Oecologia, 105*(4), 552-555. http://dx.doi.org/10.1007/bf00330019

Sturm, M., McFadden, J. P., Liston, G. E., Chapin, F. S., Racine, C. H., & Holmgren, J. (2001). Snow-shrub interactions in Arctic tundra: A hypothesis with climatic implications. *Journal of Climate, 14*(3), 336-344. http://dx.doi.org/10.1175/1520-0442(2001)014<0336:ssiiat>2.0.co;2

Tubini, N., Gruber, S., & Rigon, R. (2021). A method for solving heat transfer with phase change in ice or soil that allows for large time steps while guaranteeing energy conservation. *The Cryosphere, 15*(6), 2541-2568. https://tc.copernicus.org/articles/15/2541/2021/

Turrell, F. M., Austin, S. W., McNee, D., & Park, W. J. (1967). Thermal Conductivity of Functional Citrus Tree Wood. *Plant Physiology, 42*(8), 1025-1034. http://www.plantphysiol.org/content/plantphysiol/42/8/1025.full.pdf

Wiedmer, E., & Senn-Irlet, B. (2006). Biomass and primary productivity of an Alnus viridis stand - a case study from the Schachental valley, Switzerland. *Botanica Helvetica, 116*(1), 55-64. http://dx.doi.org/10.1007/s00035-006-0758-7

Zhang, Y.-J., Bucci, S. J., Arias, N. S., Scholz, F. G., Hao, G.-Y., Cao, K.-F., & Goldstein, G. (2016). Freezing resistance in Patagonian woody shrubs: the role of cell wall elasticity and stem vessel size. *Tree Physiology, 36*(8), 1007-1018. https://doi.org/10.1093/treephys/tpw036


**Figure 1.** Map showing the location of the Alnus-Nivus site and of the FR-Clt meteorological station near Col du Lautaret, central French Alps. Maps from https://en-gb.topographic-map.com/.

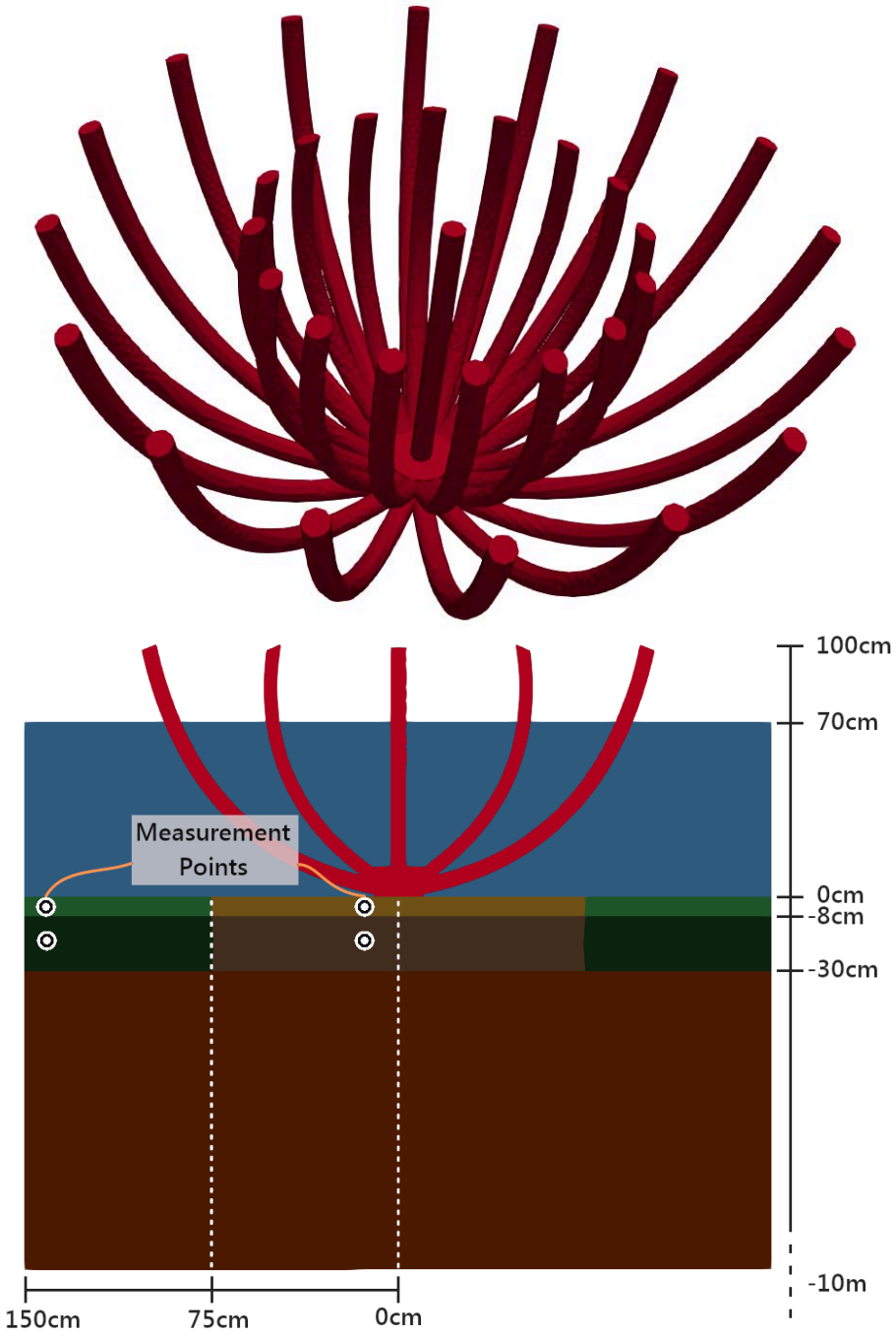


**Figure 2.** (Top) Perspective views of the alder mesh used for FEM simulations. Two concentric sets of 16 caudices 6.5 cm in diameter and 1 m high, with one extra central caudice, were used. The central trunk is 20 cm in diameter. (Bottom) Conditions for our baseline simulation. Three soil layers were used. The top two layers had different thermal properties under the alder and under the grass (Table S1). Measurement spots at 5 and 15 cm depths, and 10 and 140 cm from the center are indicated. Snow height was 70 cm.

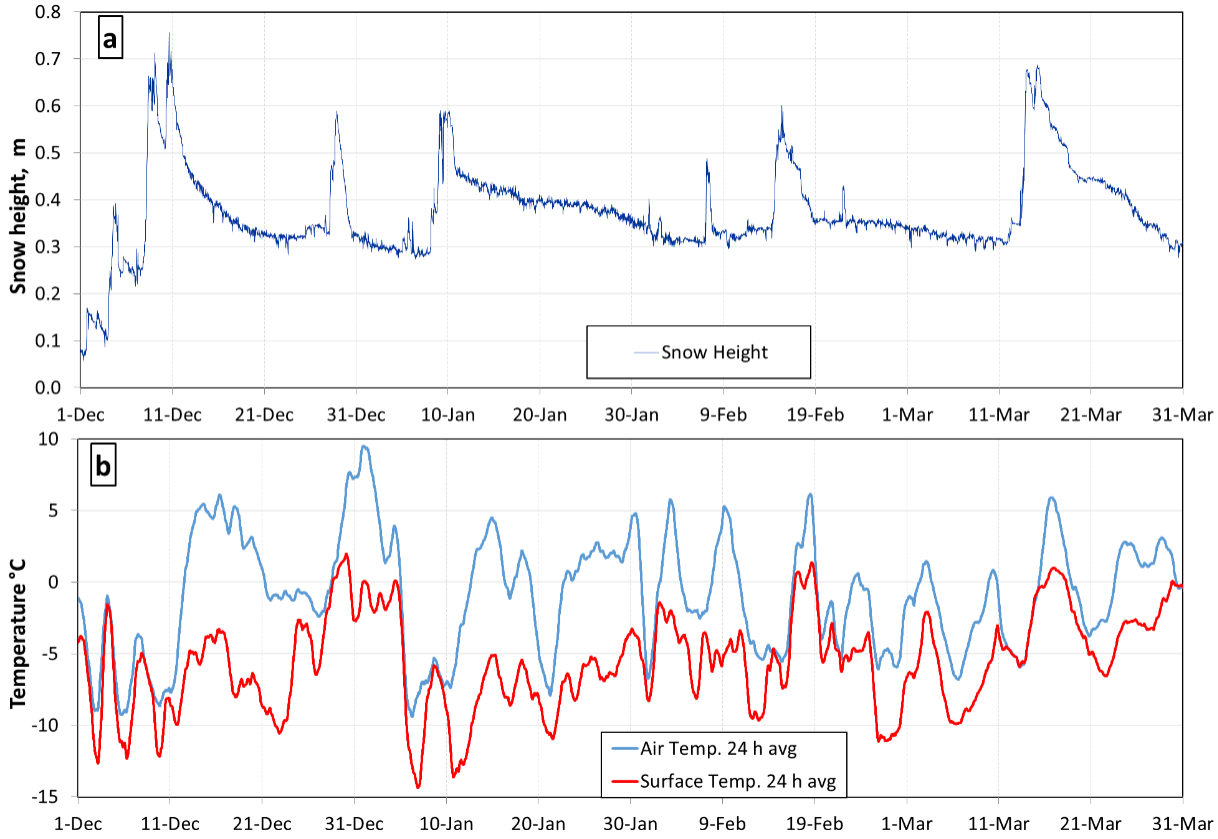


**Figure 3.** Meteorological variables measured at FR-Clt. (a) snow height; (b) 24h running-mean air and snow surface temperatures.

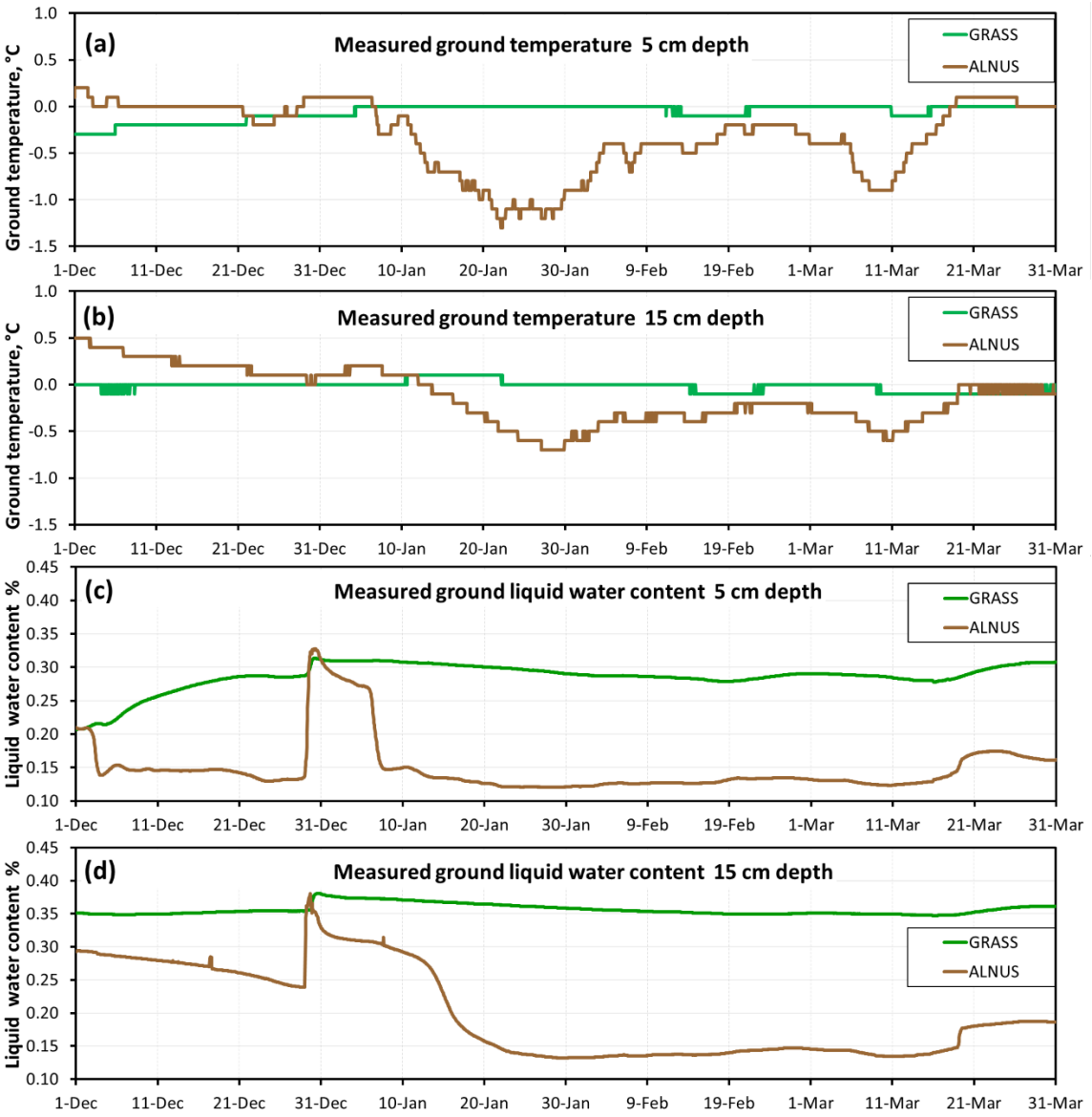


**Figure 4.** Ground temperature and volume liquid water fraction measured under alders (ALNUS) and in the nearby grass patch (GRASS). (a) temperature at 5 cm depth; (b) at 15 cm depth; (c) volume liquid water fraction at 5 cm depth; (d) at 15 cm depth.

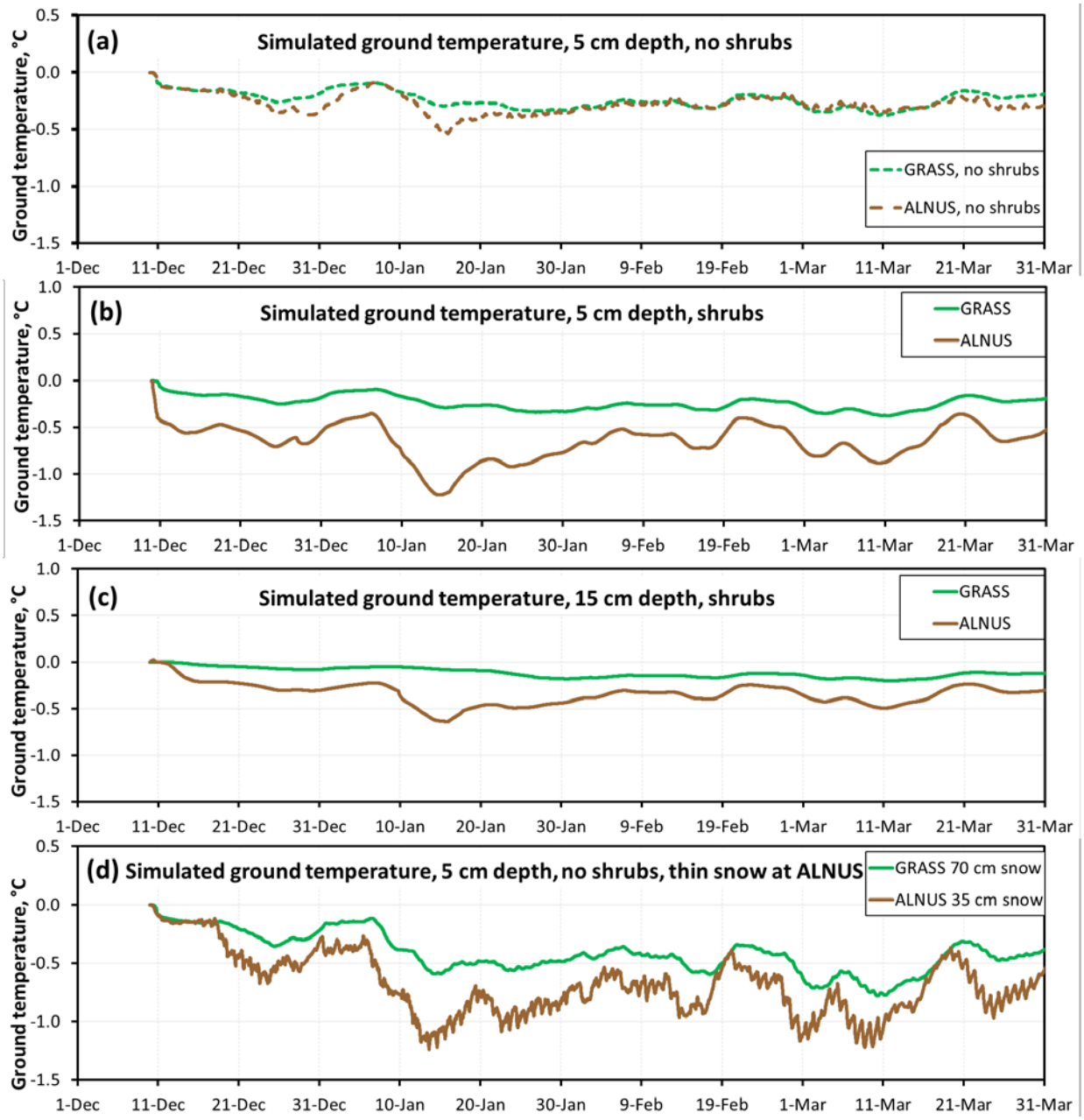


**Figure 5.** Ground temperature simulated at ALNUS and GRASS. (a) at 5 cm depth, without shrubs; (b) at 5 cm depth, with shrubs; (c) at 15 cm depth, with shrubs; (d) at 5 cm depth without shrubs and with 35 cm of snow at ALNUS and 70 cm of snow at GRASS.